

Research Article

Throughput versus Fairness: Channel-Aware Scheduling in Multiple Antenna Downlink

Eduard A. Jorswieck,¹ Aydin Sezgin,² and Xi Zhang³

¹ *Communications Laboratory, Faculty of Electrical Engineering and Information Technology, Dresden University of Technology, D-01062 Dresden, Germany*

² *Department of Electrical Engineering & Computer Science, Henry Samueli School of Engineering, University of California, Irvine, CA 92697, USA*

³ *ACCESS Linnaeus Center, Royal Institute of Technology, SE-100 44 Stockholm, Sweden*

Correspondence should be addressed to Eduard A. Jorswieck, jorswieck@ifn.et.tu-dresden.de

Received 1 July 2008; Accepted 23 December 2008

Recommended by Alagan Anpalagan

Channel aware and opportunistic scheduling algorithms exploit the channel knowledge and fading to increase the average throughput. Alternatively, each user could be served equally in order to maximize fairness. Obviously, there is a tradeoff between average throughput and fairness in the system. In this paper, we study four representative schedulers, namely the maximum throughput scheduler (MTS), the proportional fair scheduler (PFS), the (relative) opportunistic round robin scheduler (ORS), and the round robin scheduler (RRS) for a space-time coded multiple antenna downlink system. The system applies TDMA based scheduling and exploits the multiple antennas in terms of spatial diversity. We show that the average sum rate performance and the average worst-case delay depend strongly on the user distribution within the cell. MTS gains from asymmetrical distributed users whereas the other three schedulers suffer. On the other hand, the average fairness of MTS and PFS decreases with asymmetrical user distribution. The key contribution of this paper is to put these tradeoffs and observations on a solid theoretical basis. Both the PFS and the ORS provide a reasonable performance in terms of throughput and fairness. However, PFS outperforms ORS for symmetrical user distributions, whereas ORS outperforms PFS for asymmetrical user distribution.

Copyright © 2009 Eduard A. Jorswieck et al. This is an open access article distributed under the Creative Commons Attribution License, which permits unrestricted use, distribution, and reproduction in any medium, provided the original work is properly cited.

1. Introduction

The optimal strategy for maximizing the sum capacity with perfect channel state information (CSI) of a cellular single-input single-output (SISO) multiuser channel is to allow only the user having the best channel conditions in terms of SNR to transmit at each time slot (TDMA). This result in [1] has induced the notion of multiuser diversity [2], that is, the achievable capacity of the system increases with the number of the users. The corresponding scheduling policy is called maximum throughput scheduler (MTS). Subsequently, TDMA-based channel-aware scheduling schemes which consider temporal fairness [3] or stringent rate constraints under energy efficiency [4] are developed.

A major disadvantage of MTS is its unfairness toward users at the cell edge. On the other hand, the most fair but channel unaware scheduler is the round robin scheduler

(RRS) [5], that is, all transmissions take place in a strict numerical order. The MTS and RRS leave room for various channel aware schedulers that lie in between these two. In order to increase the fairness for users at the cell edge, the so-called proportional fair scheduler (PFS) can be applied. The PFS weights the instantaneous transmission rates by their averages to find the best user and achieves equal activity probability for all users [6]. Yet another scheduler, which is referred to as opportunistic round robin scheduling (ORS), was introduced in [7]. It is a combination of the RRS and MTS. The comparison of different schedulers with respect to different performance criteria is a highly viable research area. For instance, in [8], the throughput guarantee violation probability is approximated and simulated for different schedulers in different channel models. The asymptotic throughput of channel-aware schedulers is analyzed in [9].

In order to quantitatively measure the impact of the scheduler on the fairness, different measures are proposed in the literature [10–12]. The Jain fairness index (JFI) defined in [10], also known as the global fairness index (GFI) [13], provides a single number between zero and one that measures the fairness even for resource scheduling in finite windows. The average fairness defined in [11] is developed from an information theoretic point of view. The worst-case delay as it is used in, for example, [12] measures the average number of transmissions needed until all users were active at least m times.

Obviously, there exists a tradeoff between average throughput and average fairness [14]. In this paper, we study this tradeoff for the four scheduling algorithms MTS, RRS, PFS, and ORS. The main novelty lies in the systematic approach to this problem using majorization theory. This tool helps understanding the impact of user distributions within the cell on the system performance and on the average worst-case delay. The application of majorization theory allows to analytically and qualitatively assess the advantages and disadvantages of the four channel-aware schedulers. The contributions of the paper are as follows.

- (1) In Section 2.5, closed form expressions for the four scheduler for arbitrary nonsymmetrical user distributions are derived.
- (2) The impact of the user distribution on the average sum rate is analyzed in Section 3, and it is shown that the average sum rate is increased with asymmetrical user distributions for MTS. For all other schedulers (RRS, PFS, and ORS), it decreases.
- (3) Different fairness measures and their properties are discussed in Section 4. Furthermore, we study the impact of the user distribution and its connection to the service probabilities.
- (4) The asymptotic performance for high SNR or large number of users is analyzed in Section 5.
- (5) In Section 6, the sum rate of MTS, RRS, and PFS under a fixed rate constraint is derived, and the impact of user distribution is characterized.
- (6) In Section 7, we illustrate the theoretical results with numerical single-cell multiuser simulations.

The paper is concluded in Section 7. Parts of the results for single-antenna transmitter are presented without proofs in [15]. The impact of interferer locations on the downlink performance of the system is studied in [16].

2. System Model and Preliminaries

In this section, we present the system model, the channel model, the measure of the user distribution based on majorization, the high-SNR performance measures, and the four scheduler. Our approach to the cross-layer analysis of these scheduling algorithms is physical layer oriented.

2.1. System Model. In the signal model, there are K mobile users which are served by a base station in downlink transmission. The base station has multiple antennas (n_T), the mobiles have one antenna each. Denote the channels to the users as $\mathbf{h}_1, \dots, \mathbf{h}_K$. The base applies an OSTBC [17, 18] in order to exploit spatial diversity without spatial feedback overhead. Spatial feedback contains information about the spatial signatures of the user channels, whereas channel quality information contains scalar values. The data stream vectors $\mathbf{d}_1, \dots, \mathbf{d}_K$ of dimension $1 \times M$ of the K users are weighted by a power allocation p_1, \dots, p_K and added before they come into the OSTBC as $\hat{x}_1, \dots, \hat{x}_M$. The output of the OSTBC is a vector $\mathbf{x} = [x_1, \dots, x_{n_T}]$ of dimension $1 \times n_T$ (compare to system model in [19]). The code rate is given by $r_c = M/n_T$. Note that the framework can be extended also to other code classes [20].

Each mobile first performs channel matched filtering according to the effective OSTBC channel. Afterward, the received signal at user k of stream n is given by

$$y_{k,n} = a_k \sum_{l=1}^K \bar{x}_{l,n} + n_{k,n}, \quad 1 \leq n \leq M, \quad (1)$$

with fading coefficients $\alpha_k = a_k^2 = \|\mathbf{h}_k\|^2/n_T$, transmit stream n intended for user l as $\bar{x}_{l,n}$ and noise for stream n as $n_{k,n}$. There are M parallel streams for each mobile. However, all streams have the same properties in terms of a_k and noise statistics. Therefore, we restrict our attention without loss of generality to the first stream $n = 1$ and omit the index in the following. Let p_k be the power allocated to user k within one block, that is, $p_k = \mathbb{E}[|x_k|^2]$. We assume a short-term power constraint, that is, $\sum_{k=1}^K p_k \leq P$. The noise power at the receivers is σ^2 . The transmit power is distributed uniformly over the n_T transmit antennas, and each data stream has an effective power p_k/n_T . We incorporate this weighting into the transmit SNR given by $\rho = P/n_T\sigma^2$.

The mobiles feed back their scalar channel quality indicators, that is, their fading coefficient a_1, \dots, a_K to the base and we assume these numbers are perfectly known at the base station. As such, the base has perfect information about the channel norm but not about the complete fading vectors.

2.2. Channel Model. The channel vectors $\mathbf{h}_1, \dots, \mathbf{h}_K$ are modeled as independently zero-mean complex Gaussian distributed vectors with covariance matrix $c_k \mathbf{I}$ in rich multipath environment. The variance c_k depends mainly on the distance of the user to the base, and it is called average channel power. Therefore, the fading coefficients $\alpha_1, \dots, \alpha_K$ are independently χ^2 -distributed with n_T complex degrees of freedom weighted by the average channel power c_1, \dots, c_K , that is, using independent standard $\chi_{n_T}^2$ -distributed random variables w_1, \dots, w_K , the fading coefficients are expressed as $\alpha_k = c_k w_k$.

2.3. Measure of User Distribution. The distance of the mobile k to the base station is determined by the average channel power c_k . In the following, we refer to the vector of average

channel powers $\mathbf{c} = [c_1, \dots, c_K]$ as the user distribution. In order to guarantee a fair comparison between different user distributions, we constrain the sum variance to be equal to the number of users, that is, $\sum_{k=1}^K c_k = K$. Without loss of generality, we order the users in a nonincreasing way according to their fading variances, that is, $c_1 \geq c_2 \geq \dots \geq c_K$. The constraint regarding the sum of the fading variances verifies that we compare scenarios in which the channel carries the same average sum power. We need the following definitions [21].

Definition 1. For two vectors $\mathbf{x}, \mathbf{y} \in \mathbb{R}^n$, one says that the vector \mathbf{x} majorizes the vector \mathbf{y} and writes $\mathbf{x} \succ \mathbf{y}$ if $\sum_{k=1}^m x_k \geq \sum_{k=1}^m y_k$ for $m = 1, \dots, n-1$ and $\sum_{k=1}^n x_k = \sum_{k=1}^n y_k$ (note that sometimes majorization is defined by the sum of the *smallest* m components [22]).

The next definition describes a function Φ which is applied to the vectors \mathbf{x} and \mathbf{y} with $\mathbf{x} \succ \mathbf{y}$.

Definition 2. A real-valued function Φ defined on $\mathcal{A} \subset \mathbb{R}^n$ is said to be *Schur convex* on \mathcal{A} if from $\mathbf{x} \succ \mathbf{y}$ on \mathcal{A} follows $\Phi(\mathbf{x}) \geq \Phi(\mathbf{y})$. Similarly, Φ is said to be *Schur concave* on \mathcal{A} if from $\mathbf{x} \succ \mathbf{y}$ on \mathcal{A} follows $\Phi(\mathbf{x}) \leq \Phi(\mathbf{y})$.

Majorization is a useful tool to study the impact of vectors which can be partially ordered. The common monotony properties of scalar functions correspond to the Schur-convex property of vector functions. The reason for the term ‘‘Schur-convex’’ instead of ‘‘Schur-monotone’’ is that every symmetric and convex vector function is Schur-convex. Majorization is a large and active area of research in linear algebra, with entire books [21] devoted to its theory and application.

It is worth mentioning that majorization induces only a partial order on vectors with more than two components, that is, not all possible vectors can be compared with each other. This is due to the fact that vectors with more than two components cannot be totally ordered. However, a sufficient number of vectors can be compared. Also, the extreme cases can be used for comparison with any other vector. For more information about this measure of user distribution and its application see [23, Section 4.2.1].

2.4. High-SNR Measures \mathcal{S}_∞ and \mathcal{L}_∞ . The quantitative performance is analyzed using the high-SNR offset concept from [24]. Denote by $C(\rho)$ the average throughput as a function of the SNR. The two high-SNR measures are introduced as follows:

$$\begin{aligned} \mathcal{S}_\infty &= \lim_{\rho \rightarrow \infty} \frac{C(\rho)}{\log(\rho)}, \\ \mathcal{L}_\infty &= \lim_{\rho \rightarrow \infty} \left(\log(\rho) - \frac{C(\rho)}{\mathcal{S}_\infty} \right). \end{aligned} \quad (2)$$

The measures \mathcal{S}_∞ and \mathcal{L}_∞ are referred to as high-SNR slope and the high-SNR power offset, respectively. At high SNR, the average throughput behaves like $C(\rho) =$

$\mathcal{S}_\infty((\rho[\text{dB}]/3\text{dB}) - \mathcal{L}_\infty) + O(1)$. For convenience, these high-SNR measures are defined in 3 dB units. For further discussion, see [24, Section 2]. These two high-SNR measures are useful if two systems are compared which differ either in their multiplexing gain, that is, the slope of the average throughput curve at high SNR, or which have equal \mathcal{S}_∞ but are shifted at high SNR.

2.5. Types of (Channel Aware) Scheduling. Since the base station has only partial CSI in form of the channel norm, we restrict all scheduling strategies to TDMA-based scheduling. From the single-antenna downlink, it is well known that if perfect CSI is available at the base station, the sum rate is maximized by single-user transmission to the best user only [1], that is, TDMA achieves the sum capacity. This result leads to the notion of multiuser diversity and the concept of opportunistic communication [2]. This scheduler is called MTS, and the achievable average sum rate is given by

$$R_{\text{sum}}^{\text{MT}} = \mathbb{E} \left[\log \left(1 + \rho \max_{1 \leq k \leq K} \|\mathbf{h}_k\|^2 \right) \right]. \quad (3)$$

Note that the average sum rate of the MTS can be written in integral representation as

$$R_{\text{sum}}^{\text{MT}} = \int_0^\infty \frac{\rho}{1 + \rho t} \left[1 - \prod_{k=1}^K \left(1 - \frac{\Gamma(n_T, (t/c_k))}{\Gamma(n_T)} \right) \right] dt, \quad (4)$$

using the incomplete gamma function $\Gamma(a, z) = \int_z^\infty \exp(-t)t^{a-1} dt$. The case with single-antenna base and symmetrically distributed users ($\mathbf{c} = \mathbf{1}$) is studied in [25]. The MTS is unfair from a user perspective because mobiles at the cell edge have less probability to be served.

The opposite type of scheduler is the round robin scheduler (RRS). It is not channel aware but it minimizes the average worst-case delay, that is, the average time until every user has been served at least once. The average sum rate is given by

$$\begin{aligned} R_{\text{sum}}^{\text{RR}} &= \mathbb{E} \left[\frac{1}{K} \sum_{k=1}^K \log(1 + \rho \|\mathbf{h}_k\|^2) \right] \\ &= \mathbb{E} \left[\frac{1}{K} \sum_{k=1}^K \log(1 + \rho c_k w_k) \right]. \end{aligned} \quad (5)$$

Note that (5) can be rewritten for $n_T = 1$ in closed form as

$$R_{\text{sum}}^{\text{RR}} = \frac{1}{K} \sum_{k=1}^K \text{Ei} \left(1, \frac{1}{\rho c_k} \right) \exp \left(\frac{1}{\rho c_k} \right), \quad (6)$$

where the exponential integral is given by $\text{Ei}(a, x) = \int_1^\infty \exp(-tx)t^{-a} dt$.

These two schedulers are the two most extreme cases. The MTS maximizes the average sum rate, whereas the RRS minimizes the average worst-case delay. A compromise between the two is the proportional fair scheduler (PFS) [2]. For the analysis, we use the so-called relative SNR scheduler. The user is served which has the highest ratio of

the instantaneous rate to average rate. Hence, the achievable sum rate is given by

$$R_{\text{sum}}^{\text{PF}} = \mathbb{E}[\log(1 + \rho \|\mathbf{h}_{k^*}\|^2)]$$

$$\text{with } k^* = \arg \max_{1 \leq k \leq K} \frac{\|\mathbf{h}_k\|^2}{c_k}. \quad (7)$$

In reality, the average transmission rate is updated from transmission interval to transmission interval. Here, we use the ergodic formulation of the scheduler (let the window length $t_c \rightarrow \infty$). Note that (7) can be rewritten as

$$R_{\text{sum}}^{\text{PF}} = \frac{1}{K} \sum_{k=1}^K \mathbb{E}[\log(1 + \rho c_k \max_{1 \leq l \leq K} w_l)], \quad (8)$$

because the scheduling probability of all users is equal to $1/K$. For $n_T = 1$, (8) can be rewritten in closed form as

$$\frac{1}{K} \sum_{k=1}^K \sum_{l=1}^K (-1)^{l-1} \binom{K}{l} \text{Ei}\left(1, \frac{l}{\rho c_k}\right) e^{(l/\rho c_k)}. \quad (9)$$

Another interesting channel-aware scheduler is proposed in [7]. The one-round version [26] of the relative opportunistic round robin scheduler (ORS) guarantees the same average worst-case delay as the RRS but exploits a certain amount of multiuser diversity. It consists of K rounds and initializes the set of available users \mathcal{S} with $\mathcal{S} = \{1, \dots, K\}$. Within each step, the relative best user $\max_{k \in \mathcal{S}} (\|\mathbf{h}_k\|^2/c_k)$ out of the set of available users is picked and removed from the set. After K steps, it is guaranteed that all users were active at least once.

For our analysis, we need the representation in the following lemma.

Lemma 1. *The average sum rate of the ORS (13) can be written as*

$$R_{\text{sum}}^{\text{OR}} = \int_0^\infty \left[1 - \frac{1}{K^2} \sum_{n=1}^K \sum_{i=1}^K \left(1 - \frac{\Gamma(n_T, (t/c_i))}{\Gamma(n_T)} \right)^n \right]$$

$$\cdot \frac{\rho}{1 + \rho t} dt. \quad (10)$$

Proof. The CDF of the relative ORS is derived for $n_T = 1$ in [27, Equation (6)] and is given by

$$P(t) = \frac{1}{K^2} \sum_{n=1}^K \sum_{i=1}^K (1 - e^{-(t/c_i)})^n. \quad (11)$$

For general $n_T > 1$, it reads

$$P(t) = \frac{1}{K^2} \sum_{n=1}^K \sum_{i=1}^K \left(1 - \frac{\Gamma(n_T, (t/c_i))}{\Gamma(n_T)} \right)^n. \quad (12)$$

We use the integration by parts rule $\int_a^b f(x)g'(x)dx = |f(x)g(x)|_a^b - \int_a^b f'(x)g(x)dx$. Now, identify $f(x) = \log(1 + \rho x)$ and $g(x)' = p(x)$, respectively, with the pdf of the relative ORS $p(x)$. Choose carefully $g(x) = P(x) - 1$ to assure existence of the first part. Then, we obtain finally the representation in (10). \square

The sum rate performance for $n_T = 1$ can be further simplified as in [27, Equation (8)] to obtain the closed form expression

$$R_{\text{sum}}^{\text{OR}} = \frac{1}{K^2} \sum_{n=1}^K n \sum_{i=1}^K \sum_{j=0}^{n-1} \binom{n-1}{j} (-1)^j$$

$$\cdot \frac{e^{((1+j)/c_i)}}{1+j} \text{Ei}\left(1, \frac{1+j}{c_i}\right). \quad (13)$$

With the sum rate expressions in (4), (5), (8), and (10), we are now ready for the analysis of the user distribution \mathbf{c} in the next section.

3. Analysis of Sum Rate Performance

In this section, we analyze the impact of the user distribution on the sum rate performance of the four scheduler. One main question is whether the standard assumption about a symmetric user distribution, which is made often for simplification, leads to an upper or lower bound on the real system throughput. First, we present the theoretical results, and then we discuss their meaning in the paper context.

3.1. Schur-Convexity and Schur-Concavity Properties. The following result is provided in [28] for $n_T = 1$ and restated and proved here for $n_T > 1$. It states that a more asymmetrical user distribution increases the average sum rate with MTS.

Theorem 1. *Let \mathbf{c} and \mathbf{d} be two different average user powers. The average sum rate of the MTS is Schur-convex with respect to user powers \mathbf{c} and \mathbf{d} , that is,*

$$\mathbf{c} \succcurlyeq \mathbf{d} \implies R_{\text{sum}}^{\text{MT}}(\mathbf{c}) \geq R_{\text{sum}}^{\text{MT}}(\mathbf{d}). \quad (14)$$

The proof can be found in [28, Theorem 1] for the single-antenna $n_T = 1$ case. We present in Appendix A the more general proof for convenience.

The impact of the user distribution on the performance of the RRS is analyzed in the next result.

Theorem 2. *The average sum rate of the RRS is Schur-concave with respect to the vector of average user powers \mathbf{c} , that is,*

$$\mathbf{c} \succcurlyeq \mathbf{d} \implies R_{\text{sum}}^{\text{RR}}(\mathbf{c}) \leq R_{\text{sum}}^{\text{RR}}(\mathbf{d}). \quad (15)$$

Proof. Define the average sum rate as a function of \mathbf{c} as

$$R_{\text{sum}}^{\text{RR}}(\mathbf{c}) = \frac{1}{K} \sum_{k=1}^K \mathbb{E}[\log(1 + \rho c_k w_k)], \quad (16)$$

and check Schur's condition [23] directly

$$\frac{\partial R_{\text{sum}}^{\text{RR}}(\mathbf{c})}{\partial c_1} - \frac{\partial R_{\text{sum}}^{\text{RR}}(\mathbf{c})}{\partial c_2}$$

$$= \mathbb{E}\left[\frac{\rho w_1}{1 + \rho c_1 w_1}\right] - \mathbb{E}\left[\frac{\rho w_2}{1 + \rho c_2 w_2}\right] \leq 0. \quad (17)$$

\square

The impact of the user distribution on the performance of PFS is derived analogously in Theorem 3.

Theorem 3. *The average sum rate of the PFS is Schur-concave with respect to the vector of average user powers \mathbf{c} , that is,*

$$\mathbf{c} \succcurlyeq \mathbf{d} \implies R_{\text{sum}}^{\text{PF}}(\mathbf{c}) \leq R_{\text{sum}}^{\text{PF}}(\mathbf{d}). \quad (18)$$

Proof. Start from the representation in (8) and check Schur's condition

$$\begin{aligned} & \frac{\partial R_{\text{sum}}^{\text{PF}}(\mathbf{c})}{\partial c_1} - \frac{\partial R_{\text{sum}}^{\text{PF}}(\mathbf{c})}{\partial c_2} \\ &= \frac{1}{K} \mathbb{E} \left[\frac{\rho c_1 \max_{1 \leq l \leq K} w_l}{1 + \rho c_1 \max_{1 \leq l \leq K} w_l} \right] \\ & \quad - \frac{1}{K} \mathbb{E} \left[\frac{\rho c_2 \max_{1 \leq l \leq K} w_l}{1 + \rho c_2 \max_{1 \leq l \leq K} w_l} \right] \leq 0. \end{aligned} \quad (19)$$

□

Finally, the impact of the user distribution on the sum rate performance of ORS is characterized in the next result which is proved in Appendix B.

Theorem 4. *The average sum rate of the ORS is Schur-concave with respect to the vector of average user power \mathbf{c} , that is,*

$$\mathbf{c} \succcurlyeq \mathbf{d} \implies R_{\text{sum}}^{\text{OR}}(\mathbf{c}) \leq R_{\text{sum}}^{\text{OR}}(\mathbf{d}). \quad (20)$$

3.2. Discussion of Schur Properties. Let us restate the results from the last section in words. The sum rate of MTS improves with more asymmetrically distributed users. The sum rate of RRS, ORS, and PFS decreases with more asymmetrically users. Hence, the four results indicate that the common assumption about symmetrically distributed users leads to the following.

- (1) A lower bound to the sum rate performance of MTS.
- (2) An upper bound to the sum rate performance of RRS, ORS, and PFS.

This implies that a correct analysis even in terms of the sum rate does always require assumptions on the user distribution. In conclusion, there is only one scheduler which improves for asymmetrically distributed users, namely, the MTS. The average sum rates of the other scheduler, PFS, ORS, and RRS, decrease with more asymmetrically distributed user.

4. Fairness Analysis

In this section, the fairness properties of the four schedulers are analyzed. First, the average worst-case delay is proposed as a proper physical layer motivated delay measure. The impact of the service probabilities of the users on the worst-case delay is studied. Then, two other common fairness measures are reviewed, namely, Jain's fairness index and the dispersion. It is shown that all three measures are Schur-convex functions with respect to the service probabilities of the users. Finally, the connection between user distribution and service probability and delay is discussed.

4.1. Analysis of Average Worst-Case Delay. In order to capture the fairness of the different scheduler, the average worst-case delay is considered. The average worst-case delay $\mathbb{E}[D_{m,K}]$ measures the average number of transmissions that are needed until all K users have been active at least m times. We define $D_1 = \mathbb{E}[D_{1,K}]$.

The two most fair schedulers are the RRS and ORS. Both have an average worst-case delay of mK because all users are guaranteed to be active within a block of K transmissions. Especially, it takes K transmissions until every users has transmitted exactly once, that is,

$$D_1^{\text{RRS}} = D_1^{\text{ORS}} = K. \quad (21)$$

The PFS normalizes the users channels. Therefore, the probability that user k being active is, independently of k , $1 \leq k \leq K$, equal to $1/K$. Especially, it is independent of the user distribution \mathbf{c} . The result from [29] applies for $m = 1$:

$$D_1^{\text{PFS}} = K \int_0^\infty 1 - (1 - \exp(-x))^K dx. \quad (22)$$

Note that (22) can be written as

$$D_1^{\text{PFS}} = K(\Psi(K+1) + \gamma), \quad (23)$$

with the Ψ -function [30, 6.3] and Euler's constant γ [30, 6.1.3].

The analysis of the MTS is more difficult. Rewrite the average worst-case delay [12, Section 3.3] without dropping probability as

$$D_1^{\text{MTS}} = n \int_0^\infty \left(1 - \prod_{k=1}^K \left(1 - \frac{\Gamma(m, d_k t)}{\Gamma(m)} \right) \right) dt. \quad (24)$$

For $m = 1$, the expression in (24) says how many packets are transmitted on average until every user has at least transmitted one. The coefficients d_k in (24) are related to the probability that user k is chosen $\pi_k = d_k/K$. For the MTS, we prove the following result.

Theorem 5. *The average worst-case delay $\mathbb{E}[D_{1,K}]$ is Schur-convex with respect to \mathbf{d} , that is,*

$$\mathbf{d}_1 \succcurlyeq \mathbf{d}_2 \implies D_1^{\text{MTS}}(\mathbf{d}_1) \geq D_1^{\text{MTS}}(\mathbf{d}_2). \quad (25)$$

Proof. In order to check Schur's condition, [23] consider

$$\begin{aligned} & \frac{\partial \mathbb{E}[D_{1,K}](\mathbf{d})}{\partial d_1} - \frac{\partial \mathbb{E}[D_{1,K}](\mathbf{d})}{\partial d_2} \\ &= n \int_0^\infty \prod_{l=3}^K (1 - \exp(-d_l t)) g(t, d_1, d_2) dt, \end{aligned} \quad (26)$$

with $g(t, d_1, d_2) = t \exp(-d_2 t) (1 - \exp(-d_1 t)) - t \exp(-d_1 t) (1 - \exp(-d_2 t)) \geq 0$ for all $d_1 \geq d_2$, and $t \geq 0$. It follows that the integral in (24) is greater than or equal to zero. □

Theorem 5 formally states the intuitive fact that the average worst-case delay grows if some users are less frequent

active on average. If the probability that user k is active is equal to $1/K$, independently of k , then the expression in (24) is minimized. Note that a similar analysis has been performed in the different context of birthday matching in [31].

4.2. Jain's Fairness Index and Dispersion. In [10], a quantitative measure of fairness is introduced. It is called Jain's fairness index (JFI) or global fairness index (GFI) [13]. Define x_k as the amount of a resource that is distributed to user k . Then, JFI is defined as [10, Equation (2)]

$$\text{JFI} = \frac{((1/K)\sum_{k=1}^K x_k)^2}{(1/K)\sum_{k=1}^K x_k^2}. \quad (27)$$

Let us specialize this general definition to the case in which one resource is one transmission. The JFI is averaged over L transmissions [27]

$$\text{JFI}(L) = \frac{\mathbb{E}_L((1/K)\sum_{k=1}^K x_k)^2}{\mathbb{E}_L(1/K)\sum_{k=1}^K x_k^2}. \quad (28)$$

Denote by π_k the probability that user k is active within L transmissions, then $x_k = \pi_k L$. Collect $\boldsymbol{\pi} = [\pi_1, \dots, \pi_K]$. Let $L \rightarrow \infty$ to obtain the long-term average JFI as

$$\text{JFI} = \frac{((1/K)\sum_{k=1}^K \pi_k)^2}{(1/K)\sum_{k=1}^K \pi_k^2}. \quad (29)$$

Note that $\sum_{k=1}^K \pi_k = 1$, and hence (29) leads to the dispersion of $\boldsymbol{\pi}$:

$$\text{Dsp}(\boldsymbol{\pi}) = \frac{1}{\sum_{k=1}^K \pi_k^2}. \quad (30)$$

Interestingly, this measure of fairness is closely related to majorization theory. The function in (30) is symmetric and concave in $\boldsymbol{\pi}$ and therefore Schur concave [23, Proposition 2.8]. A function is called symmetric if the argument vector can be arbitrarily permuted without changing the value of the function.

Corollary 1. *The dispersion is a Schur-concave function of the vector $\boldsymbol{\pi}$, that is,*

$$\boldsymbol{\pi}_1 \succcurlyeq \boldsymbol{\pi}_2 \implies \text{Dsp}(\boldsymbol{\pi}_1) \leq \text{Dsp}(\boldsymbol{\pi}_2). \quad (31)$$

4.3. Connection of User Distribution, Service Probability, and Delay. From the results in the last sections, it follows that the impact of the user location on the different fairness measures depends on the resulting service probability vector $\boldsymbol{\pi}$. Therefore, we have to map the user distribution vector \mathbf{c} to the service probability vector $\boldsymbol{\pi}$. The concrete mapping depends on the chosen scheduler. For PFS, the service probabilities of all users are equal to $\pi_k = 1/K$ and thus independent of \mathbf{c} .

In order to apply majorization theory to the analysis of the average worst-case delay as a function of the user

distribution, we have to transfer the partial order for user distributions to the partial order for probability that a user k is picked.

Define the vector of probabilities that user k is picked $\boldsymbol{\pi}$ as a function of the user distribution \mathbf{c} , that is,

$$\begin{aligned} \pi_k(\mathbf{c}) &= \Pr\left[c_k w_k \geq \max_{l \neq k} c_l w_l\right] \\ &= \sum_{\boldsymbol{\pi} \in \mathcal{P} \setminus k} \int_{a_{\pi_{K-1}}=0}^{\infty} \int_{a_{\pi_{K-2}}=a_{\pi_{K-1}}}^{\infty} \cdots \\ &\quad \cdot \int_{a_k=a_{\pi_1}}^{\infty} \prod_{k=1}^K \frac{a_k^{n_T-1} e^{-(a_k/\Gamma(n_T)c_k)}}{c_k} d\mathbf{a}. \end{aligned} \quad (32)$$

The RHS in (32) contains all possible disjunct events, that is, all permutations, such that $c_k w_k \geq c_{\pi_1} w_{\pi_1} \geq c_{\pi_2} w_{\pi_2} \geq \cdots \geq c_{\pi_{K-1}} w_{\pi_{K-1}}$. The sum over all probabilities, that is, integrals with certain limits, gives the probability that user k is picked.

Unfortunately, the next result is an impossibility result. It shows that it is not possible to say that if $\mathbf{c} \succcurlyeq \mathbf{d}$ then automatically $\boldsymbol{\pi}(\mathbf{c}) \succcurlyeq \boldsymbol{\pi}(\mathbf{d})$.

Corollary 2. *The mapping from the vector of user distributions to the vector of service probabilities is not order preserving with respect to the partial order majorization.*

Proof. We provide a counterexample. Consider the user distribution vectors $\mathbf{c} = [5, 3, 2]^T$ and $\mathbf{d} = [4, 4, 2]^T$ and $n_T = 1$. The resulting activity probabilities computed according to (32) are given by $\boldsymbol{\pi}(\mathbf{c}) = [0.6428, 0.1786, 0.1786]^T$ and $\boldsymbol{\pi}(\mathbf{d}) = [0.4167, 0.4167, 0.1666]^T$. Majorization cannot be used to compare these two vectors because $\pi_1(\mathbf{c}) > \pi_1(\mathbf{d})$ but $\pi_1(\mathbf{c}) + \pi_2(\mathbf{c}) < \pi_1(\mathbf{d}) + \pi_2(\mathbf{d})$. \square

Even though the connection between user distribution and service probability is not order preserving with respect to the partial order of majorization, it does not imply that the average worst-case delay is not a Schur-convex or Schur-concave function of the user distribution. Due to the complicated dependency of the average worst-case delay and the user distribution via (32), the following observation is stated as a conjecture.

Conjecture 1. *The average worst-case delay of MTS as a function of the user distribution is Schur-convex, that is, $\mathbf{c} \succcurlyeq \mathbf{d} \implies \mathbb{E}[D_{1,K}(\mathbf{c})] \geq \mathbb{E}[D_{1,K}(\mathbf{d})]$.*

5. Asymptotic Characterizations

In this section, we characterize the average sum rate of the different scheduling schemes for high SNR or for a large number of users. The scaling laws of the schemes are derived as a function of the user distribution. These results provide more quantitative but closed form expressions for the sum rate performance of the four schedulers.

5.1. *High-SNR Behavior.* The high-SNR slope \mathcal{S}_∞ as defined in (2) for all four scheduling schemes is equal to one because

$$\begin{aligned}\mathcal{S}_\infty &= \lim_{\rho \rightarrow \infty} \frac{\int_0^\infty \log(1 + \rho x) pdf(x) dx}{\log(\rho)} \\ &= \int_0^\infty \lim_{\rho \rightarrow \infty} \frac{\log(1 + \rho x)}{\log(\rho)} pdf(x) dx \\ &= \int_0^\infty pdf(x) dx = 1.\end{aligned}\quad (33)$$

It is allowed to swap integration and limit by applying the dominated convergence theorem. In general, any TDMA scheme could have at most a high-SNR slope of one. The high-SNR power offset is different for the four schedulers. It is derived in the following result.

Theorem 6. *The high-SNR power offset is characterized for four cases as follows.*

- (1) For MTS, the high-SNR power offset is bounded from below and above by

$$\begin{aligned}\gamma + \log(\Gamma(1 + n_T)^{1/n_T}) - \sum_{k=1}^K (-1)^{k-1} \binom{Kn_T}{k} \log(k) \\ \geq \mathcal{L}_\infty^{\text{MT}} \geq \gamma - \log(Kn_T).\end{aligned}\quad (34)$$

For $n_T = 1$, the lower bound in (34) is equal to the lower bound result in [23, Theorem 2].

- (2) For RRS, the high-SNR power offset as a function of the user distribution is given by

$$\mathcal{L}_\infty^{\text{RR}}(\mathbf{c}) = \frac{1}{K} \sum_{k=1}^K -\Psi(n_T) - \log(c_k).\quad (35)$$

For $n_T = 1$, we obtain the closed form expression (compare to [15])

$$\mathcal{L}_\infty^{\text{RR}}(\mathbf{c}) = \frac{1}{K} \sum_{k=1}^K \gamma - \log(c_k).\quad (36)$$

- (3) For PFS, the high-SNR power offset as a function of the user distribution is given by

$$\mathcal{L}_\infty^{\text{PF}}(\mathbf{c}) = -\Psi(n_T) - \frac{1}{K} \sum_{k=1}^K \sum_{l=1}^K (-1)^{l-1} \binom{K}{l} \log\left(\frac{l}{c_k}\right).\quad (37)$$

- (4) For ORS, the high-SNR power offsets as a function of the user distribution is given by

$$\begin{aligned}\mathcal{L}_\infty^{\text{OR}}(\mathbf{c}) &= \frac{1}{K^2} \sum_{n=1}^K n \sum_{k=1}^K \sum_{j=0}^{n-1} \binom{n-1}{j} \frac{(-1)^j}{1+j} \\ &\cdot \left(\gamma + \log\left(\frac{1+j}{c_k}\right) \right).\end{aligned}\quad (38)$$

The proof of Theorem 6 follows similar lines as in [32, Theorem 2] and is, therefore, omitted. Note that the Schur convexity of (36) can be directly observed and this approves the result in (15). However, in (37) and (38), the Schur convexity cannot be directly observed because of the alternating sum.

The high-SNR power offsets fulfill the following inequality chain:

$$\mathcal{L}_\infty^{\text{MT}} \leq \{\mathcal{L}_\infty^{\text{PF}}, \mathcal{L}_\infty^{\text{OR}}\} \leq \mathcal{L}_\infty^{\text{RR}}.\quad (39)$$

The order of PFS and ORS depends on the user distribution and number of antennas at the base station scenario. Note that the average worst-case delay does not scale with the SNR.

5.2. *Scaling with Number of Users.* First, consider the case in which the users are symmetrically distributed, that is, $\mathbf{c} = \mathbf{1}$. The scaling behavior with $K \rightarrow \infty$ for fixed SNR ρ can be easily shown by considering a simple upper and lower bounds on the average sum rate. The average sum rate of RR does not scale with K at all.

Corollary 3. *For symmetrically distributed users $\mathbf{c} = \mathbf{1}$, the average sumrates of MTS, PFS, and ORS scale for large K with $\log(K)$, that is,*

$$\begin{aligned}\lim_{K \rightarrow \infty} \frac{R_{\text{sum}}^{\text{MT}}(K)}{\log(K)} &= \lim_{K \rightarrow \infty} \frac{R_{\text{sum}}^{\text{PF}}(K)}{\log(K)} \\ &= \lim_{K \rightarrow \infty} \frac{R_{\text{sum}}^{\text{OR}}(K)}{\log(K)} = 1.\end{aligned}\quad (40)$$

The case in which the users are not symmetrically distributed is discussed in the numerical results section. The scaling of the average worst-case delay with the number of users is also of interest and is thus studied in Corollary 4. It follows directly from (21) and (23).

Corollary 4. *For symmetrically distributed users, the average worst-case delay scales linearly with K for RRS and ORS. For MTS and PFS, it scales as $K \log(K)$, that is,*

$$\begin{aligned}\lim_{K \rightarrow \infty} \frac{D_1^{\text{RRS}}(K)}{K} &= \lim_{K \rightarrow \infty} \frac{D_1^{\text{ORS}}(K)}{K} = 1, \\ \lim_{K \rightarrow \infty} \frac{D_1^{\text{MTS}}(K)}{K \log(K)} &= \lim_{K \rightarrow \infty} \frac{D_1^{\text{PFS}}(K)}{K \log(K)} = 1.\end{aligned}\quad (41)$$

The case in which the users are not symmetrically distributed is discussed also in the numerical results section. Note that the scaling law for MTS and PFS in (41) is the best case as shown in Theorem 5, the case in which the users are symmetrically distributed offers the lowest average worst-case delay.

6. Fixed Rate Allocation and Long-Term Power Constraint

In this section, we consider a certain communication scenario which leads to a slightly modified performance

function on the physical layer. Usually, the traffic is divided into classes (see, e.g., traffic classes in [33]) which require a certain SNR level to guarantee successful delivery of the user contents. In the following, we study the behavior of the sum rate under fixed rate allocations for the three schedulers (MTS, RRS, and PFS) as a function of the user distribution for comparison with the sum rate behavior from the last section.

Let us assume that we have only one fixed transmission rate R_0 available, and each scheduled user obtains its information packet with that rate. Therefore, a certain SNR is needed for successful transmission. Denote the long-term sum transmit power constraint at the base station as P_ℓ , that is,

$$\mathbb{E}_{a_1, \dots, a_k} \left[\sum_{k=1}^K p_k(a_1, \dots, a_k) \right] \leq P_\ell. \quad (42)$$

We consider the three schedulers MTS, RRS, and PFS. The power allocation at the base station for all three schedulers is channel inversion under the long-term power constraint.

Theorem 7. *The achievable sum rate for fixed rate transmission of the RRS is given by*

$$R_{\text{sum},fx}^{\text{RR}} = \frac{1}{K} \sum_{k=1}^K \log \left(1 + \frac{\rho P_\ell}{\mathbb{E}[(1/c_k w_k)]} \right). \quad (43)$$

The achievable sum rate for fixed rate transmission of the MTS is given by

$$R_{\text{sum},fx}^{\text{MT}} = \log \left(1 + \frac{\rho P_\ell}{\mathbb{E}[(1/\max_{1 \leq k \leq K} c_k w_k)]} \right). \quad (44)$$

Finally, the sum rate for fixed rate transmission of the PFS is given by

$$R_{\text{sum},fx}^{\text{PF}} = \frac{1}{K} \sum_{k=1}^K \log \left(1 + \frac{\rho P_\ell}{\mathbb{E}[(1/c_k \max_{1 \leq k \leq K} w_k)]} \right). \quad (45)$$

Proof. We will use one framework to derive the achievable sum rate for fixed rate transmission [34]. Denote the instantaneous channel power of the scheduled user as ζ . Then, the instantaneous achievable rate is $\log(1 + \rho \zeta p(\zeta))$ with power $p(\zeta)$ allocated. This instantaneous rate should be equal to the fixed rate R_0 under the average power constraint in (42). We solve

$$R_0 = \log(1 + \rho \zeta p(\zeta)) \quad (46)$$

for $p(\zeta)$ and normalize the constant c_P with respect to the long-term power constraint to obtain the optimal power allocation

$$p(\zeta) = \frac{c_P}{\zeta} = \frac{P_\ell}{\zeta} \frac{1}{\mathbb{E}[1/\zeta]}. \quad (47)$$

Equation (47) is simply channel inversion with long-term power constraint, that is,

$$\mathbb{E}[p(\zeta)] = P_\ell \mathbb{E} \left[\frac{1}{\zeta} \right] \frac{1}{\mathbb{E}[1/\zeta]} = P_\ell. \quad (48)$$

Inserting (47) into (46) yields

$$R_0 = \log \left(1 + \rho \frac{P_\ell}{\mathbb{E}[1/\zeta]} \right). \quad (49)$$

Then expressions in (43), (44), and (45) follow when we use the effective channels ζ after scheduling. \square

The impact of the user location on the sum rate performances is characterized in the following corollary.

Corollary 5. *The sum rate of RRS with fixed rate constraint is Schur concave with respect to \mathbf{c} . The sum rate of PFS with fixed rate constraint is Schur concave with respect to \mathbf{c} .*

The sum rates with fixed rate constraint and long-term power constraint for RRS and PFS show the same behavior as the sum rate with short-term power constraint.

Proof. We verify indirectly Schur's condition for the RRS and PFS and thereby leave the expectation unsolved. Both sum rates R_0^{PF} and R_0^{RR} can be written as functions of the user distribution \mathbf{c}

$$\psi(\mathbf{c}) = \frac{1}{K} \sum_{k=1}^K \log \left(1 + \frac{\rho c_k P_\ell}{\mathbb{E}[x]} \right) \quad (50)$$

for some random variable x . The function in (50) is symmetric with respect to \mathbf{c} . The sum of concave functions in c_k is Schur-concave (see, e.g., [23, Proposition 2.7] or [21, 3.C.1]). \square

Regarding the impact of the user distribution on the MTS sum rate with fixed rates, we observe that the behavior depends on the number of antennas and number of users. We leave this for future research.

7. Numerical Simulations

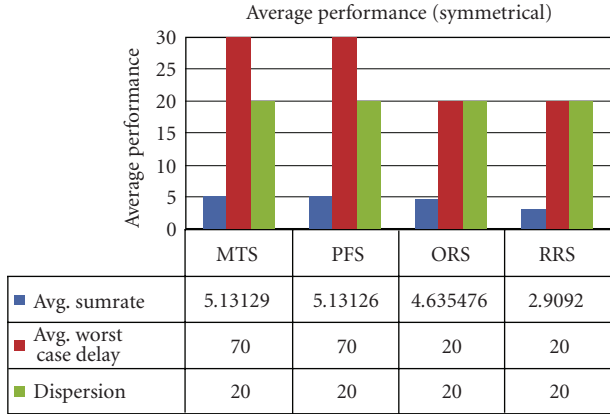
In this section, we present illustrations which validate and explain the theoretical results from the last sections. The performance for the case with symmetrically distributed users $\mathbf{c} = \mathbf{1}$ is compared to the case with asymmetrically users. For the asymmetrically user distribution, we choose the exponential decaying model

$$c_k = \exp(-tk), \quad \text{and normalize } \sum_{k=1}^K c_k = K. \quad (51)$$

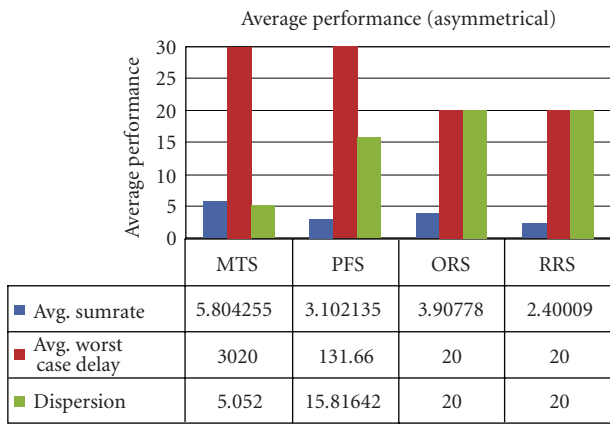
For $K = 20$ and $t = 0.2$, we obtain the user distribution

$$\mathbf{c} = [3.6930, 3.0236, 2.4755, 2.0268, 1.6594, 1.3586, \\ 1.1123, 0.9107, 0.7456, 0.6105, 0.4998, 0.4092, \\ 0.3350, 0.2743, 0.2246, 0.1839, 0.1505, 0.1232, \\ 0.1009, 0.0826]. \quad (52)$$

In the numerical simulations, for each data point, 100 000 Monte Carlo runs are performed to compute the averages.



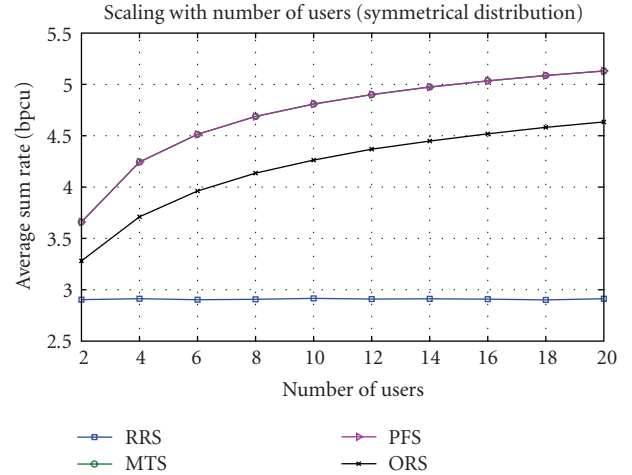
(a)



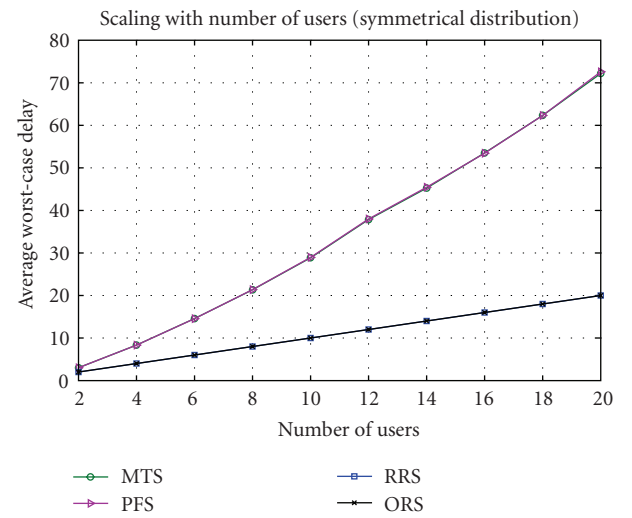
(b)

FIGURE 1: Average sum rate, worst-case delay, and dispersion for $K = 20$ symmetrically and asymmetrically distributed users.

7.1. General Results. In Figure 1, the average sum rate, the average worst-case delay, and the dispersion are shown for the four studied schedulers. In Figure 1(a), the users are symmetrically distributed, that is, $\mathbf{c} = \mathbf{1}$, whereas in Figure 1(b), the users are asymmetrically distributed according to the model in (51) with $t = 0.2$. The results in Figure 1 illustrate the following observations. The average sum rate of MTS increases with more asymmetrically distributed users (compare to (14)), while the average sum rate of all three other schedulers decreases (compare to (15), (18), and (20)). However, PFS outperforms ORS for the symmetrical scenario, whereas it is the other way round for the asymmetrical scenario. Another observation is that the average worst-case delay is more differentiated than the dispersion. This underlines that the average worst-case delay is better suited for fairness analysis than the JFI-based dispersion. Finally, the average worst-case delay for the asymmetrical scenario of the PFS and ORS tends to grow without bound. Therefore, taking the tradeoff between fairness and average sum rate into account, the PFS and ORS perform reasonable well. PFS is advantageous in symmetric scenarios whereas ORS performs better in asymmetric scenarios.



(a)



(b)

FIGURE 2: Average sum rate and worst-case delay versus number of users for symmetrically distributed users.

7.2. Scaling with Number of Users. In Figures (2) and (3), we show the average performance of the four scheduling algorithms for symmetrically distributed as well as asymmetrically distributed users. The derived scaling laws in (40) and (41) are confirmed. The interesting observation is that for the asymmetrical case, PFS outperforms OFS for a small number of users, whereas it is the other way round for large number of users.

The average worst case delay for MTS and PFS increases with asymmetrical user distribution as predicted in Theorem 5. As soon as a single c_k approaches zero, the average worst-case delay approaches infinity. The round-based schedulers RRS and ORS are robust against the asymmetrical user distribution.

The main observation in this section is that for practical scenarios in which fairness is important as well as users are randomly distributed within the cell, ORS clearly outperforms PFS. Note that the results presented here hold for a

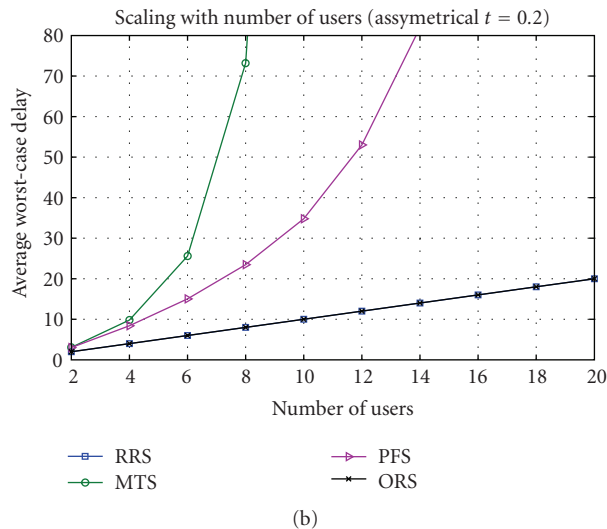
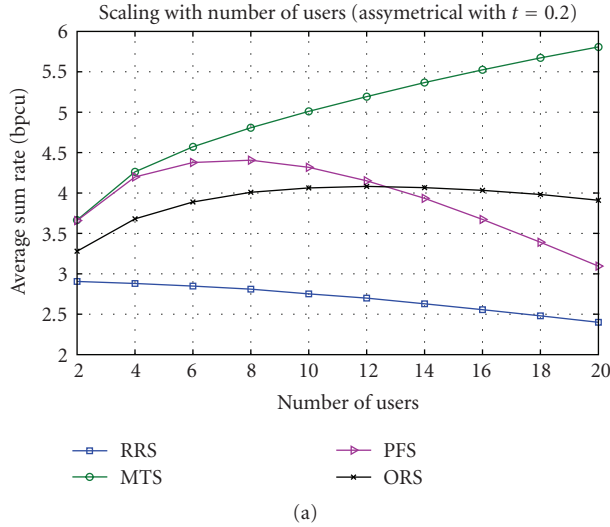


FIGURE 3: Average sum rate and worst-case delay versus number of users for asymmetrically distributed users.

static scenario in which we place the users only once inside the cell and simulate the small-scale fading. Mobility as well as traffic models is left for further research.

7.3. Multiple Antenna Case—OSTBC. The application of OSTBC yields to a tradeoff between the code rate and the number of degrees of freedom of the channel gain. The code rate r_C decreases with the number of antennas, whereas the number of degrees of freedom of the χ^2 distributed channel gain increases. For an OSTBC with n_T transmit antennas, it is shown in [35] that the maximum achievable code rate is given by

$$r_C(n_T) = \frac{\lfloor (n_T + 1)/2 \rfloor + 1}{2 \lfloor (n_T + 1)/2 \rfloor}. \quad (53)$$

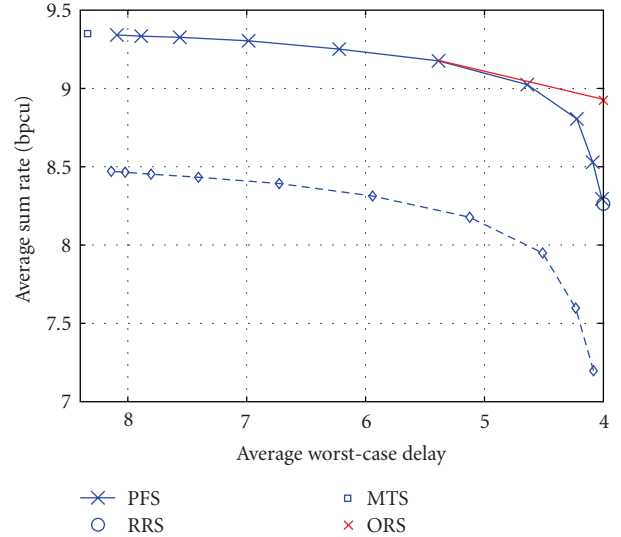


FIGURE 4: Average sum rate/worst-case delay tradeoff, $n_T = \{1, 2\}$; $K = 4$; $\text{SNR} = 20$ dB.

The code rate $r_C(n_T)$ starts at $r_C(1) = r_C(2) = 1$ and decreases to $\lim_{n_T \rightarrow \infty} r_C(n_T) = 1/2$. Therefore, we restrict the numerical simulations to the case $n_T = 2$.

In Figure 4, the achievable average sum rate versus average worst-case delay tradeoff is shown for a two antenna BS with four users at $\text{SNR} = 20$ dB for the four schedulers. The PFS is operated at ten window length operating points $t_c = 2^k$, $k = 1, \dots, 10$. The RRS has lowest delay, whereas the MTS has largest delay but best performance. The closure of the convex hull of all operating points gives the achievable sum rate/delay region. The dashed line shows the single-antenna case. It can be observed that two antennas increase average sum rate as well as decrease the average worst-case delay significantly. Note that no additional (spatial) feedback is required to achieve this gain.

8. Conclusions

In this paper, we proposed an approach to analyze qualitatively the tradeoff between system throughput and fairness in a multiuser multiple antenna downlink transmission system. Four representative (three of them channel aware) schedulers were studied for different user distributions using majorization theory. The sum rate of MTS improves with asymmetrically user distribution, whereas the sum rate of all other schedulers improves with symmetrically user distribution. MTS and RRS serve as upper and lower bounds on throughput and lower and upper bounds on worst-case delay, respectively. The throughput-delay tradeoff of the four schedulers is characterized; if fairness as well as performance is important, the optimal choice will depend on the user distribution and the number of users. Finally, the gain of using multiple antennas without increased feedback overhead at the base station is illustrated.

Appendices

A. Proof of Theorem 1

Proof. In the proof, we verify Schur's condition directly. Therefore, we need the first derivative of $R_{\text{sum}}^{\text{MT}}$ with respect to c_1 and c_2 given as

$$\begin{aligned} \frac{\partial R_{\text{sum}}^{\text{MT}}}{\partial c_1} &= \int_0^\infty \frac{\rho t}{1 + \rho t} \prod_{k=3}^K \left(1 - \frac{\Gamma(n_T, (t/c_k))}{\Gamma(n_T)} \right) \\ &\quad \cdot \left(1 - \frac{\Gamma(n_T, (t/c_2))}{\Gamma(n_T)} \right) \frac{(t^{n_T-1}/c_1)}{c_1^2 \Gamma(n_T)} \exp\left(-\frac{t}{c_1}\right) dt, \\ \frac{\partial R_{\text{sum}}^{\text{MT}}}{\partial c_2} &= \int_0^\infty \frac{\rho t}{1 + \rho t} \prod_{k=3}^K \left(1 - \frac{\Gamma(n_T, (t/c_k))}{\Gamma(n_T)} \right) \\ &\quad \cdot \left(1 - \frac{\Gamma(n_T, (t/c_1))}{\Gamma(n_T)} \right) \frac{(t^{n_T-1}/c_2)}{c_2^2 \Gamma(n_T)} \exp\left(-\frac{t}{c_2}\right) dt. \end{aligned} \quad (\text{A.1})$$

Define the two functions

$$\begin{aligned} f(\rho, t, \mathbf{c}) &= \frac{\rho t}{1 + \rho t} \prod_{k=3}^K \left(1 - \frac{\Gamma(n_T, (t/c_k))}{\Gamma(n_T)} \right), \\ g(t, c_1, c_2) &= \left(1 - \frac{\Gamma(n_T, (t/c_2))}{\Gamma(n_T)} \right) \frac{(t/c_1)^{n_T-1}}{c_1^2 \Gamma(n_T)} \exp\left(-\frac{t}{c_1}\right) \\ &\quad - \left(1 - \frac{\Gamma(n_T, (t/c_1))}{\Gamma(n_T)} \right) \frac{(t/c_2)^{n_T-1}}{c_2^2 \Gamma(n_T)} \exp\left(-\frac{t}{c_2}\right), \end{aligned} \quad (\text{A.2})$$

in order to express the difference of the first derivatives of the sum rate of the MTS as

$$\frac{\partial R_{\text{sum}}^{\text{MT}}}{\partial c_1} - \frac{\partial R_{\text{sum}}^{\text{MT}}}{\partial c_2} = \int_0^\infty f(\rho, t, \mathbf{c}) g(t, c_1, c_2) dt. \quad (\text{A.3})$$

The following properties of the functions f and g are easily verified; f is monotonic increasing from zero to one. The function g is $g(t=0) = 0$, has one zero at $t^* : g(t^*) = 0$, and is negative for all $t < t^*$ and positive for all $t > t^*$. Therefore, we can lower bound (A.3) by using the zero t^* as

$$\frac{\partial R_{\text{sum}}^{\text{MT}}}{\partial c_1} - \frac{\partial R_{\text{sum}}^{\text{MT}}}{\partial c_2} \geq f(\rho, t^*, \mathbf{c}) \int_0^\infty g(t, c_1, c_2) dt. \quad (\text{A.4})$$

Finally, the integral in (A.4) can be computed in closed form

$$\begin{aligned} \int_0^\infty g(t, c_1, c_2) dt &= \frac{1}{2 c_1 c_2 \Gamma(1 + n_T) \sqrt{\pi}} \\ &\quad \cdot \left\{ 2\sqrt{\pi} \Gamma(n_T + 1) [c_2 - c_1] + \Gamma(n_T + 1/2) 4^{n_T} \left(\frac{c_1}{c_2} \right)^{n_T} \right. \\ &\quad \cdot \left[c_1 \cdot {}_2F_1\left(n_T, 2n_T; 1 + n_T; -\left(\frac{c_1}{c_2}\right)\right) \right. \\ &\quad \left. \left. - c_2 \cdot {}_2F_1\left(n_T, 2n_T; 1 + n_T; -\left(\frac{c_2}{c_1}\right)\right) \right] \right\}, \end{aligned} \quad (\text{A.5})$$

where ${}_2F_1(a, b; c; z)$ is the Gauss hypergeometric function [30, Chapter 15]. For single-antenna BS, we set $n_T = 1$ to obtain

$$G(c_1, c_2, 1) = 0, \quad (\text{A.6})$$

which is in perfect agreement with the result and its proof in [28]. Since, the function $G(c_1, c_2, n_T)$ is monotonic increasing with n_T , this implies that

$$\frac{\partial R_{\text{sum}}^{\text{MT}}}{\partial c_1} - \frac{\partial R_{\text{sum}}^{\text{MT}}}{\partial c_2} \geq f(\rho, t^*, \mathbf{c}) G(c_1, c_2, n_T) \geq 0, \quad (\text{A.7})$$

which verifies Schur's condition for Schur convexity. \square

B. Proof of Theorem 4

Proof. The proof is similar to the proof in Appendix A. The difference is that we have two sums in the integral instead of the product. Starting from the representation in (10), the difference of the first partial derivatives with respect to c_1 and c_2 , respectively, is computed

$$\begin{aligned} \frac{\partial R_{\text{sum}}^{\text{OR}}}{\partial c_1} &= \int_0^\infty \frac{\rho}{1 + \rho t} \frac{1}{K^2} \\ &\quad \cdot \sum_{k=1}^K \frac{(1 - (\Gamma(n_T, t/c_1)/\Gamma(n_T)))^k k t^{n_T} \exp(-t/c_1)}{\Gamma(n_T) - \Gamma(n_T, t/c_1) c_1^{n_T+1}} dt, \\ \frac{\partial R_{\text{sum}}^{\text{OR}}}{\partial c_2} &= \int_0^\infty \frac{\rho}{1 + \rho t} \frac{1}{K^2} \\ &\quad \cdot \sum_{k=1}^K \frac{(1 - (\Gamma(n_T, t/c_2)/\Gamma(n_T)))^k k t^{n_T} \exp(-t/c_2)}{\Gamma(n_T) - \Gamma(n_T, t/c_2) c_2^{n_T+1}} dt. \end{aligned} \quad (\text{B.1})$$

Define the two functions

$$\begin{aligned} \phi(\rho, t) &= \frac{\rho}{1 + \rho t}, \\ \gamma(t, c_1, c_2, k, n_T) &= \frac{(1 - (\Gamma(n_T, t/c_1)/\Gamma(n_T)))^k k t^{n_T} \exp(-t/c_1)}{\Gamma(n_T) - \Gamma(n_T, t/c_1) c_1^{n_T+1}} \\ &\quad - \frac{(1 - (\Gamma(n_T, t/c_2)/\Gamma(n_T)))^k k t^{n_T} \exp(-t/c_2)}{\Gamma(n_T) - \Gamma(n_T, t/c_2) c_2^{n_T+1}}, \end{aligned} \quad (\text{B.2})$$

in order to rewrite the difference of the first derivatives as

$$\begin{aligned} \Delta &= \frac{\partial R_{\text{sum}}^{\text{OR}}}{\partial c_1} - \frac{\partial R_{\text{sum}}^{\text{OR}}}{\partial c_2} \\ &= \frac{1}{K^2} \sum_{k=1}^K \int_0^\infty \phi(\rho, t) \gamma(t, c_1, c_2, k, n_T) dt. \end{aligned} \quad (\text{B.3})$$

The properties of the functions ϕ and γ are as follows. ϕ is monotonic decreasing with respect to t , and γ has similar properties as the function g in the proof in Appendix A.

$\gamma(t=0) = 0$, it has on zero at $t^* : g(t^*) = 0$, it is negative for all $t < t^*$ and positive for all $t > t^*$. Therefore, we obtain an upper bound on Δ in (B.3) as

$$\Delta \leq \frac{1}{K^2} \sum_{k=1}^K \phi(\rho, t^*) \int_0^\infty \gamma(t, c_1, c_2, k, n_T) dt = 0, \quad (\text{B.4})$$

because $\int_0^\infty \gamma(t, c_1, c_2, k, n_T) dt = 0$. This verifies Schur's condition for Schur concavity and completes the proof. \square

References

- [1] R. Knopp and P. A. Humblet, "Information capacity and power control in single-cell multiuser communications," in *Proceedings of IEEE International Conference on Communications (ICC '95)*, vol. 1, pp. 331–335, Seattle, Wash, USA, June 1995.
- [2] D. Tse and P. Viswanath, *Fundamentals of Wireless Communication*, Cambridge University Press, Cambridge, UK, 2005.
- [3] T. Issariyakul and E. Hossain, "ORCA-MRT: an optimization-based approach for fair scheduling in multirate TDMA wireless networks," *IEEE Transactions on Wireless Communications*, vol. 4, no. 6, pp. 2823–2835, 2005.
- [4] X. Wang, A. G. Marques, and G. B. Giannakis, "Power-efficient resource allocation and quantization for TDMA using adaptive transmission and limited-rate feedback," *IEEE Transactions on Signal Processing*, vol. 56, no. 9, pp. 4470–4485, 2008.
- [5] F. Halsall, *Data Communications, Computer Networks and Open Systems*, Electronic Systems Engineering, Addison-Wesley, Reading, Mass, USA, 4th edition, 1996.
- [6] L. Yang and M.-S. Alouini, "Performance analysis of multiuser selection diversity," *IEEE Transactions on Vehicular Technology*, vol. 55, no. 6, pp. 1848–1861, 2006.
- [7] S. S. Kulkarni and C. Rosenberg, "Opportunistic scheduling policies for wireless systems with short term fairness constraints," in *Proceedings of IEEE Global Telecommunications Conference (GLOBECOM '03)*, vol. 1, pp. 533–537, San Francisco, Calif, USA, December 2003.
- [8] V. Hassel, G. E. Øien, and D. Gesbert, "Throughput guarantees for wireless networks with opportunistic scheduling: a comparative study," *IEEE Transactions on Wireless Communications*, vol. 6, no. 12, pp. 4215–4220, 2007.
- [9] G. Song and Y. Li, "Asymptotic throughput analysis for channel-aware scheduling," *IEEE Transactions on Communications*, vol. 54, no. 10, pp. 1827–1834, 2006.
- [10] R. Jain, D. Chiu, and W. Hawe, "A quantitative measure of fairness and discrimination for resource allocation in shared computer systems," Research Report TR-301, DEC, New York, NY, USA, September 1984.
- [11] R. Elliott, "A measure of fairness of service for scheduling algorithms in multiuser systems," in *Proceedings of the Canadian Conference on Electrical and Computer Engineering (CCECE '02)*, vol. 3, pp. 1583–1588, Winnipeg, Canada, May 2002.
- [12] M. Sharif and B. Hassibi, "Delay considerations for opportunistic scheduling in broadcast fading channels," *IEEE Transactions on Wireless Communications*, vol. 6, no. 9, pp. 3353–3363, 2007.
- [13] N. Golmie, *Coexistence in Wireless Networks*, Cambridge University Press, Cambridge, UK, 2007.
- [14] Z. Han and K. J. R. Liu, *Resource Allocation for Wireless Networks: Basics, Techniques, and Applications*, Cambridge University Press, Cambridge, UK, 2008.
- [15] E. A. Jorswieck, A. Sezgin, and X. Zhang, "Framework for analysis of opportunistic schedulers: average sum rate vs. average fairness," in *Proceedings of the 4th Workshop on Resource Allocation in Wireless Networks (RAWNET '08)*, Berlin, Germany, March 2008.
- [16] A. Sezgin, E. Jorswieck, and M. Charafeddine, "Interaction between scheduling and user locations in an OSTBC coded downlink system," in *Proceedings of the 7th International ITG Conference on Source and Channel Coding (SCC '08)*, Ulm, Germany, January 2008.
- [17] S. M. Alamouti, "A simple transmit diversity technique for wireless communications," *IEEE Journal on Selected Areas in Communications*, vol. 16, no. 8, pp. 1451–1458, 1998.
- [18] V. Tarokh, H. Jafarkhani, and A. R. Calderbank, "Space-time block codes from orthogonal designs," *IEEE Transactions on Information Theory*, vol. 45, no. 5, pp. 1456–1467, 1999.
- [19] E. Jorswieck, B. Ottersten, A. Sezgin, and A. Paulraj, "Guaranteed performance region in fading orthogonal space-time coded broadcast channels," *EURASIP Journal on Wireless Communications and Networking*, vol. 2008, Article ID 268979, 12 pages, 2008.
- [20] A. Sezgin and E. Jorswieck, "On the performance of partial feedback based orthogonal block coding," in *Proceedings of the 62nd IEEE Vehicular Technology Conference (VTC '05)*, vol. 3, pp. 1504–1508, Dallas, Tex, USA, September 2005.
- [21] A. W. Marshall and I. Olkin, *Inequalities: Theory of Majorization and Its Application*, vol. 143 of *Mathematics in Science and Engineering*, Academic Press, New York, NY, USA, 1979.
- [22] R. A. Horn and C. R. Johnson, *Matrix Analysis*, Cambridge University Press, Cambridge, UK, 1985.
- [23] E. Jorswieck and H. Boche, "Majorization and matrix-monotone functions in wireless communications," *Foundations and Trends in Communications and Information Theory*, vol. 3, no. 6, pp. 553–701, 2006.
- [24] A. Lozano, A. M. Tulino, and S. Verdú, "High-SNR power offset in multiantenna communication," *IEEE Transactions on Information Theory*, vol. 51, no. 12, pp. 4134–4151, 2005.
- [25] C.-J. Chen and L.-C. Wang, "A unified capacity analysis for wireless systems with joint multiuser scheduling and antenna diversity in Nakagami fading channels," *IEEE Transactions on Communications*, vol. 54, no. 3, pp. 469–478, 2006.
- [26] M. Johansson, "Diversity-enhanced equal access—considerable throughput gains with 1-bit feedback," in *Proceedings of the 5th IEEE Workshop on Signal Processing Advances in Wireless Communications (SPAWC '04)*, pp. 6–10, Lisbon, Portugal, July 2004.
- [27] V. Hassel, M. R. Hanssen, and G. E. Øien, "Spectral efficiency and fairness for opportunistic round robin scheduling," in *Proceedings of IEEE International Conference on Communications (ICC '06)*, vol. 2, pp. 784–789, Istanbul, Turkey, July 2006.
- [28] E. A. Jorswieck and H. Boche, "Throughput analysis of cellular downlink with different types of channel state information," in *Proceedings of IEEE International Conference on Communications (ICC '06)*, vol. 4, pp. 1526–1531, Istanbul, Turkey, July 2006.
- [29] D. J. Newman and L. Shepp, "The double dixie cup problem," *The American Mathematical Monthly*, vol. 67, no. 1, pp. 58–61, 1960.
- [30] M. Abramowitz and I. A. Stegun, *Handbook of Mathematical Functions*, Dover, New York, NY, USA, 1970.
- [31] M. L. Clevenston and W. Watkins, "Majorization and the birthday inequality," *Mathematics Magazine*, vol. 64, no. 3, pp. 183–188, 1991.

- [32] E. A. Jorswieck, P. Svedman, and B. Ottersten, "Performance of TDMA and SDMA based opportunistic beamforming," *IEEE Transactions on Wireless Communications*, vol. 7, no. 11, pp. 4058–4063, 2008.
- [33] T. Bonald and A. Proutire, "On the traffic capacity of cellular data networks," in *Proceedings of the 24th International Conference on Thermoelectrics (ICT '05)*, Clemson, SC, USA, June 2005.
- [34] E. A. Jorswieck and H. Boche, "Delay-limited capacity: multiple antennas, moment constraints, and fading statistics," *IEEE Transactions on Wireless Communications*, vol. 6, no. 12, pp. 4204–4208, 2007.
- [35] X.-B. Liang, "Orthogonal designs with maximal rates," *IEEE Transactions on Information Theory*, vol. 49, no. 10, pp. 2468–2503, 2003.